Supporting Information for

Multi-objective ensemble-processing strategies to optimize the simulation of the western North Pacific Subtropical High in boreal summer

Cenxiao Sun[1], Zhihong Jiang[1*], Zhenfei Tang[1,2] & Laurent Li[3]

[1] *Key Laboratory of Meteorological Disaster of Ministry of Education (KLME), Collaborative Innovation Center on Forecast and Evaluation of Meteorological Disaster, Nanjing University of Information Science and Technology, Nanjing, China*

[2] *Fujian Climate Center, Fujian Province Meteorology Bureau, Fuzhou, China*

[3] *Laboratoire de Météorologie Dynamique, IPSL, CNRS, Sorbonne Université, Ecole Normale Supérieure, Ecole Polytechnique, Paris, France*

Corresponding Author: Zhihong Jiang, zhjiang@nuist.edu.cn

Contents of this file

Introduction

This supporting information includes detailed introduction of methods (Text S1-S3), list of CMIP6 models used in this study (Table S1) and the evidence (Figure S1-S7) to support out arguments in the main text. Figure S1 provides the diagrammatic sketch of the Pareto-optimal and Least-distance strategy scheme. Figure S2 shows the observed SLP and inter-model standard deviation of simulated SLP bias to determine the constrain area. Figure S3 shows the observed relationships between SLP and SST at interannual scale based on a Singular Value Decomposition (SVD) analysis. Figure S4 gives the RMSE of four objectives of the Pareto-optimal and Least-distance strategy, and the histogram of RMSE simulated by Pareto-optimal subsets is shown in Figure S5. Figure S6 and S7 provide the climatology and biases of SLP and SST simulated by CMIP6-MME, Pareto-optimal, Least-distance strategy and Rank-based Weighting scheme during validation period.

Text S1. Least-distance strategy over Pareto-optimality

The Least-distance strategy is used to further constrain Pareto-optimal subsets. Taking the constraining of two variables (A and B) as an example, the process is given schematically in Figure.S1. The actual practice consists of the following steps:

The thresholds of RMSE for variables A and B are firstly determined, represented by a and b in Figure S1, as the 90th percentile from the Pareto front. The point with minimum RMSE, represented by (a_0, b_0), is then taken as the center of an ellipse with a-a_0 and b-b_0 as its major and minor axis. All Pareto-optimal dots (red triangles in Figure S1) within the ellipse are those selected. That is, a selected dot (x, y) satisfies $\frac{(x-a0)^2}{(a-a0)^2}+\frac{(y-b0)^2}{(b-b0)^2}<1$, shown by purple triangles in Figure S1. It can be seen that in this way the Pareto-optimal subsets are further constrained by additional conditions stipulating least distances to the observation (the coordinate origin).

Text S2. Rank-based weighting method

The rank of model *i* for its simulation of variable *j* ($S_{i,j}$) can be obtained by sorting its RMSE from smallest to largest, smaller rank indicating better model performance. The quality metric R of model *i* is represented as a function of its ranking position:

$$R_i = \frac{\sum_i^n \sum_j^m S_{i,j}}{\sum_j^m S_{i,j}}$$

where n and m designate the number of CMIP6 models and geophysical variables, respectively. Then the weight (W_i) of model *i* can be calculated by:

$$W_i = \frac{R_i}{\sum_i^n R_i}$$

In fact, W_i can be seen as the normalized value of R_i (Chen et al., 2011).

Text S3. Taylor diagram and Taylor skill score

The Taylor diagram provides three aspects of statistical information: pattern correlation coefficient, centered RMSE, and the ratio of spatial standard deviation. A good simulation would present that both the pattern correlation coefficient and the ratio of standard deviations are close to 1, and the centered RMSE is close to 0 (Taylor, 2001).

And TSS is used to summarize the measures of the Taylor diagram, calculated as:

$$TSS = \frac{4(1+R)^2}{\left(\frac{\sigma_o}{\sigma_m} + \frac{\sigma_m}{\sigma_o}\right)^2 (1+R_0)^2}$$

where R is the spatial correlation coefficient between simulation and observation, R_0 is the maximum correlation coefficient attainable (here we use 0.999); σ_m and σ_o are the spatial standard deviations of the simulated and observed spatial patterns, respectively. The closer the value of TSS to 1, the better the agreement between simulation and observation.

Table S1 Basic information of CMIP6 models used in this work.

Number	**Model**	**Atmos. Resolution** (#lat×#lon)	**Ocean. Resolution** (#lat×#lon)
1	ACCESS-CM2	144×192	300×360
2	ACCESS-ESM1-5	145×192	300×360
3	BCC-CSM2-MR	160×320	232×360
4	CAS-ESM2-0	128×256	196×360
5	CMCC-ESM2	192×288	292×362
6	CNRM-CM6-1	128×256	180×360
7	CNRM-ESM2-1	128×256	180×360
8	E3SM-1-1-ECA	180×360	180×360
9	E3SM-1-1	180×360	180×360
10	EC-Earth3-Veg-LR	160×320	292×362
11	EC-Earth3	256×512	292×362
12	FGOALS-g3	80×180	218×360
13	GFDL-ESM4	180×288	576×720
14	HadGEM3-GC31-MM	324×432	1205×1440
15	IITM-ESM	94×192	200×360
16	INM-CM5-0	120×180	180×360
17	MIROC6	128×256	256×360
18	MPI-ESM1-2-HR	192×384	404×802
19	MPI-ESM1-2-LR	96×192	220×256
20	MRI-ESM2-0	160×320	363×360
21	NorESM2-LM	96×144	385×360
22	TaiESM1	192×288	384×320

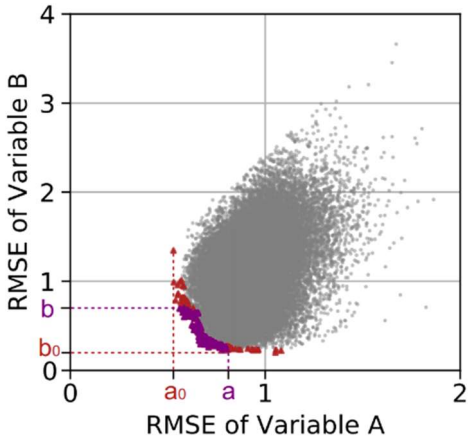

Figure S1. A diagrammatic sketch of Pareto-optimal and Least-distance strategy scheme. The RMSE in all subsets, Pareto-optimal and Least-distance strategy are shown as dense grey dots, red and purple triangles. Note that some red triangles are overlayed by purple ones. a_0 and b_0 represent the minimum RMSE value, and a and b represent the threshold of RMSE in variable A and B, respectively.

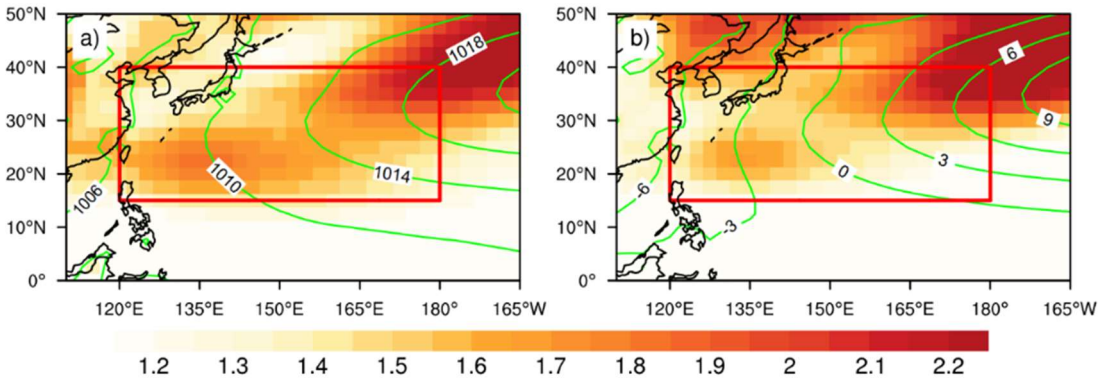

Figure S2. (a) Simulated standard deviation of inter-model biases in CMIP6 (shadings) and observed (green contours) SLP climatology in boreal summer (JJA) for the whole historical period (1961-2014) (Units: hPa). (b) is the same as in (a), but for SLP with 0-40°N zonal mean subtracted. The red boxes (15-40°N, 120-180°E) indicate our target SLP region.

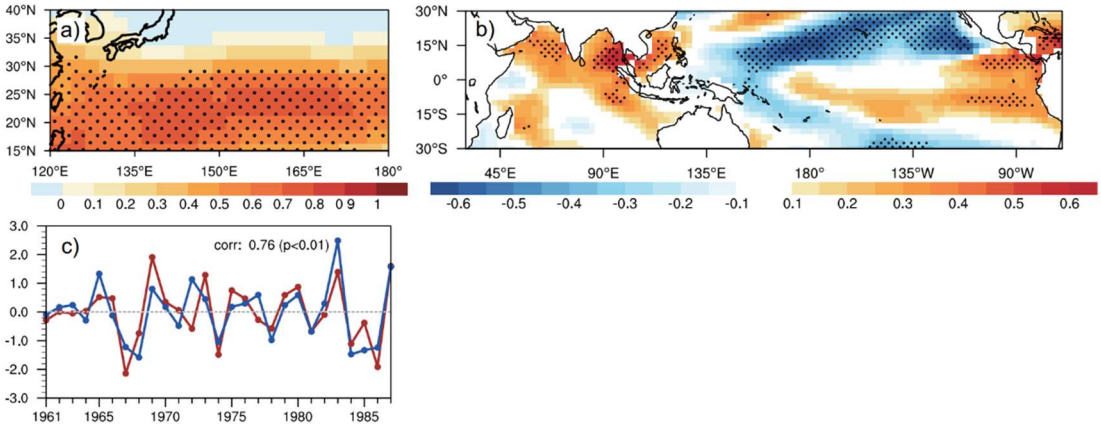

Figure S3. Leading Singular Value Decomposition heterogeneous correlation maps for the standardized pre-processed SLP (a) and tropical Indo-Pacific SST (b) in the observation during the calibration period (1961-1987) boreal summer. Dotted areas represent statistically significant correlations according to a 10% level two-sample t-test. (c) The standardized corresponding principal components of SLP (red line) and SST (blue line), and the correlation coefficient and p-value are marked at the top right. The gray line shows the value of 0.

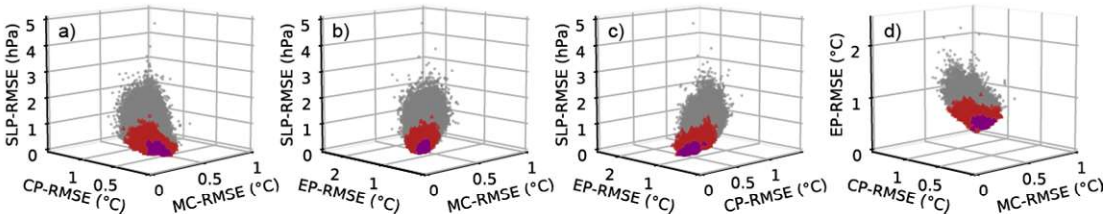

Figure S4. The RMSE of climatology for SLP, MC-SST, CP-SST and EP-SST in all subsets (gray dots), Pareto-optimal (red triangles) and Least-distance strategy subsets (purple triangles), relative to observations during calibration period (1961-1987). Due to the drawing limitation of 4-demision image, only its projection on 3-demision plots is shown.

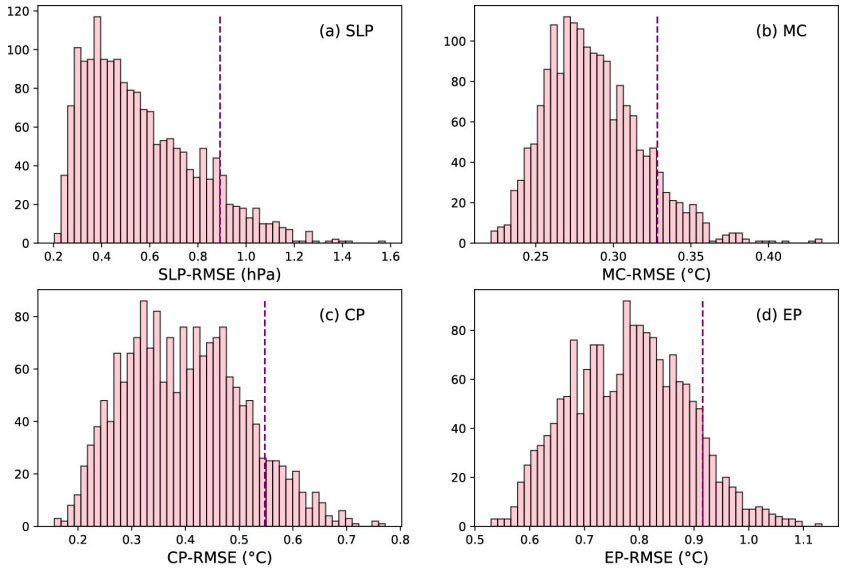

Figure S5. The histogram of RMSE simulated by Pareto-optimal subsets. The ordinate represents the number of subsets, purple lines represent the 90th of RMSE.

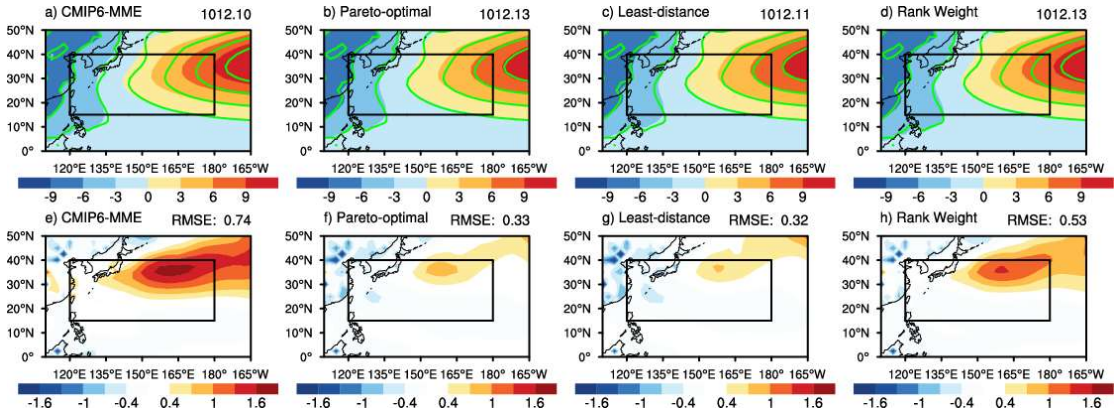

Figure S6. The spatial distribution of pre-processed SLP climatology (a-d) and bias (e-h) of boreal summer in validation period simulated by CMIP6-MME, Pareto-optimal scheme, Least-distance strategy and Rank-based weighting scheme. The black boxes represent the constrained SLP area. Green contours in a-e represent the SLP climatology of observation, numbers on the top right represent the zonal mean SLP between 0-40°N. And numbers on the top right in f-j represent the RMSE of constrained SLP area (Units: hPa).

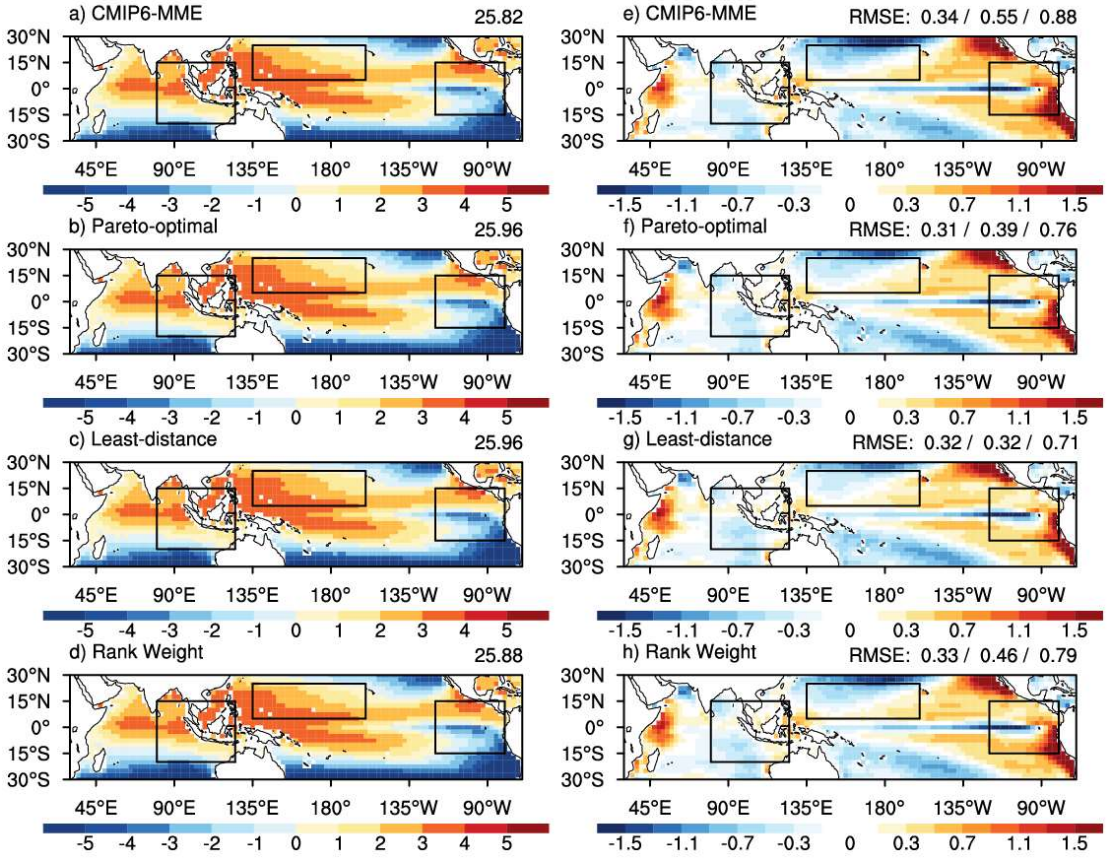

Figure S7. The spatial distribution of pre-processed SST climatology (a-d) and bias (e-h) of boreal summer in validation period simulated by CMIP6-MME, Pareto-optimal scheme, Least-distance strategy and Rank-based weighting scheme during validation period. The black boxes represent the constrained SST region. Numbers on the top right in a-d represent the areal-mean SST over the studied basin (30°S-30°N, 30°E-70°W). And numbers on the top right in f-j represent the RMSE of MC/CP/EP-SST, respectively (Units: °C).

Reference:

Chen, W., Jiang, Z. & L., Li. (2011). Probabilistic projections of climate change over China under the SRES A1B scenario using 28 AOGCMs. *Journal of Climate*, 24(17), 4741–4756. https://doi.org/10.1175/2011JCLI4102.1

Taylor, K. (2001). Summarizing multiple aspects of model performance in a single diagram. Journal of Geophysical Research: Atmosphere, 106(D7), 7183−7192, https://doi.org/10.1029/2000JD900719.